

FREQUENTIST AND BAYESIAN APPROACH FOR THE MIXTURE CURE MODELS WITH GENERALIZED POWER GENERALIZED WEIBULL BASELINE: AN APPLICATION TO CANCER DATA

BEATRICE AMIN NJAU¹, SAMUEL MUSILI MWALILI² and GEORGE OTIENO ORWA²

¹Department of Mathematics (Statistics option) Programme, Pan African University, Institute for Basic Sciences, Technology and Innovation (PAUSTI), Nairobi, 62000-00200, Kenya.

²Department of Statistics and Actuarial Sciences, Jomo Kenyatta University of Agriculture and Technology, Nairobi 62000-00200, Kenya.

Abstract

This paper develops the Weibull distribution by adding a new parameter to the classical distribution, the generalized power generalized Weibull mixture cure model distribution, and it's extremely useful when modeling survival data with parameter hazard rate function shape. As a result, there is greater flexibility in analyzing and modeling various data types. The essential mathematical and statistical characteristics of the proposed distribution are generated. In this paper. Many well-known life time special sub-models, such as Rayleigh, Power generalized Weibull, Nadarajah-Haghighi, Weibull, and Exponential, are included in the proposed distribution. The maximum likelihood distribution method was used to estimate the unknown parameters of the proposed distribution; and the effectiveness of the estimators was determined using Markov Chain Monte Carlo simulation study. The Markov Chain Monte Carlo used to develop diagnostic methods. This distribution is important because it can model non-monotone and monotone, upside-down bathtub, and bathtub hazard rate functions. All of which are widely used in survival and efficiency data analysis. Moreover, the flexibility and effectiveness of the proposed distribution are demonstrated in a real-world data set and compared to its sub models. Based on the goodness of fit and information criterion value, the proposed distribution is accurate. Finally, the estimation of the data set is determined using Bayesian inference and Gibb's sampling performance. In addition to Bayes estimates, the highest posterior density reliable intervals and Markov Chain Monte Carlo convergence diagnostic technique were used.

Keywords: Bathtub, Bayesian, Classical Approach, Hazard Rate, Maximum Likelihood Estimation, Monotonic and Non-Monotonic.

1. INTRODUCTION

Inconsistency and survival studies, applied statisticians use a variety of probability distributions. The distributions can be used in a variety of disciplines, including engineering, medicine, economics, industrial and physical fields, and many others (Muse et al., 2021). The most commonly used distributions in survival and consistency analysis are gamma distributions, exponential distribution, Weibull distributions, generalized exponential distributions, generalized gamma distributions, log-logistic distributions, extreme value distributions, log-normal distributions, generalized Weibull distributions and Burr XII distributions (Muse et al., 2021). (Bagdonavicius & Nikulin, 2001), suggested the three-parameter power generalization of the Weibull distribution, by adding a shape parameter.

The power generalized Weibull distribution's cumulative density function and probability density function are shown;

$$G(t) = 1 - \exp\{1 - (1 + \xi t^\phi)^\omega\}, \phi, \xi, \omega, t > 0 \quad (1)$$

$$\text{And } g(t) = \xi\phi\omega t^{(\phi-1)}(1 + \xi t^\phi)^{1-\omega} \exp\{1 - (\xi t^\phi)^\omega\}, \phi, \xi, \omega, t > 0 \quad (2)$$

Where ϕ and ω are two shape parameters ξ is a scale parameter, respectively. When $\omega=1$, the normal Weibull distribution is a special case of one. This is also an extended form of the exponential distributions (Selim, 2018),(Muse et al., 2021),(Zhang & Xie, 2007). The power generalized Weibull distribution's hazard rate function is good and flexible. This distribution is commonly used in the development of accelerated failure time models. The chi-square goodness of fit test was also used to show that a PGW first analyzed the randomized censored survival time's data from patients enrolled in a head and neck cancer clinical trial. (HAGHIGHI, 2009), (Nikulin & Haghighi, 2006),(Gupta et al., 1998). In this paper, we focus on a GPGW with a mixture cure model modification, which, while similar in shape to the PGW distribution, is better suited for use in survival data analysis when focusing on censored observations, which are usual in survival data. Since the survival functions are complicated (Selim, 2018),(Muse et al., 2021), the presence of missing data makes the use of Weibull or exponential models difficult. Nonetheless, since logarithms of very small positive numbers give a large negative numbers, the Weibull distribution may overestimate very short survival times (Muse et al., 2021). We will concentrate on the GPGW Mixture cure model because its hazard rate shows the above said behavior.

(Gupta et al., 1998), Presented the exponentiated method, which is one of the most well-known and oldest method for generalizing probability distributions. If $\hat{S}(t) = [1 - S(t)]$ and $S(t)$ are the survival and cumulative density function of the baseline distribution, respectively, then CDF of exponentiated distribution family of Lehmann type II is defined as one minus, β power of $\hat{S}(t)$

$$F(T) = 1 - \hat{S}(T)^\beta \quad (3)$$

As well as the respective probability density function (pdf)

$$f(t) = \beta z(t) \hat{S}(T)^{\beta-1} \quad (4)$$

Where $z(t)$ indicates the baseline distribution's pdf. As a result, in this study, we suggest a cure fraction model that has a more adjustable survival time distribution for the latent variable (Omer et al., 2020). In this paper, we contrast the effectiveness of the GPGW mixture cure model and its sub-models, which are based on the GPGW-MCM and are applied to various forms of the failure rate function. In the colon data set, for example, which is accessible in the R package colonDC, we consider the presence of hazard function shapes, parameter estimation, and parameter performance (convergences). The parameters were estimated using the Bayesian method (De Pascoa, et al., 2011).

2. THE COLON DATA

Colorectal cancer (CRC), the third most common malignancy and the second most lethal cancer is expected to cause 1.9 million new cases and 0.9 million deaths worldwide in 2020 (Xi & Xu, 2021). CRC is more common in developed countries, and its prevalence is rising in middle and lower income countries as a result of westernization. Furthermore, there is an increasing incidence of CRC with an early onset. The high number of CRC cases is posing an increasing global public health challenge (Xi & Xu, 2021). Boosting CRC awareness is critical for promoting healthy lifestyle choices, novel CRC action plans, and the implementation of global detection methods, all of which are crucial to reducing CRC morbidity and mortality in the future. Even though the largest part of colon patients are cured by their primary treatment, it is impossible to distinguish them from uncured patients (Xi & Xu, 2021), (Omer et al., 2020). As a result, accurate estimation of the likelihood of cure is critical in order to plan further treatment to enhance the survival of uncured colon cancer patients' citeomer2020cure. We suggest colon data from R colonDC in the Survival package, on Cancer, obtained from a clinical trial, in this study. A total of 929 patients were included in this trial, with 49% being exposed to the treatment and the remaining individuals being right-censored.

3. GPGW_{MCM} (EXPONENTIATED POWER GENERALIZED WEIBULL DISTRIBUTION MIXTURE CURE MODEL)

The reliability function $S(t)$ of the generalized power generalized Weibull distribution model is simply the β^{th} power of the reliability function of power generalized Weibull distribution as follows,

$$S(t) = [\exp\{1 - (1 + \xi t^\phi)^\omega\}]^\beta, \phi, \xi, \omega, \beta > 0, t \geq 0 \quad (5)$$

$$F(t) = 1 - S(t) = 1 - \exp\{\beta[1 - (1 + \xi t^\phi)^\omega]\}, \phi, \xi, \omega, \beta, > 0, t > 0 \quad (6)$$

And the associated probability density function is

$$f(t) = \phi \xi \omega \beta t^{\phi-1} (1 + \xi t^\phi)^{\omega-1} \exp\{\beta[1 - (1 + \xi t^\phi)^\omega]\}, \phi, \xi, \omega, \beta > 0, t > 0 \quad (7)$$

Where ξ and β are scale parameters, and ϕ and ω are shape parameters. Because the Weibull distribution is a special case of exponentiated (Gupta et al., 1998) when $\omega = \beta = 1$, it can also be regarded as a generalization of the Weibull distribution.

3.1 Fundamental properties of $S(t)$ and hazard function $\lambda(t)$

$S(0)$ equals 1 and $S(1)$ equals infinity (∞). $S(t)$ is a function that does not increase. $N(t)$ the number of events that occurred in $(0, t)$ $\text{Pois}(\lambda, t)$ (Beatrice, Samuel, & George, 2022) As a result, $S_{\text{MCM}}(t)$ of the generalized power generalized Weibull distribution mixture cure model is given as;

$$S_{\text{MCM}}(t) = \zeta + (1 - \zeta)S(t) \quad (8)$$

The associated pdf is;

$$f_{MCM}(t) = (1 + \zeta)f(t) \tag{9}$$

3.2 Some GPGW-MCM distribution special distributions

Nadarajah-Haghighi (NH), Rayleigh (R), Weibull (W) and power generalized Weibull (PGW) mixture cure modes distributions are sub-models of the GPGW mixture cure modes distributions. Table 1 shows sub-models of the $GPGW_{MCM}$ distribution for various parameter values.

Table 1: Table of $GPGW_{MCM}$ distribution and its sub-models

Models	ζ	ϕ	ω	ξ	β
$GPGW_{MCM}$	$\sqrt{\quad}$	$\sqrt{\quad}$	$\sqrt{\quad}$	$\sqrt{\quad}$	$\sqrt{\quad}$
PGW_{MCM}	$\sqrt{\quad}$	$\sqrt{\quad}$	$\sqrt{\quad}$	$\sqrt{\quad}$	1
W_{MCM}	$\sqrt{\quad}$	$\sqrt{\quad}$	1	$\sqrt{\quad}$	1
R_{MCM}	$\sqrt{\quad}$	2	1	$\sqrt{\quad}$	1
NH_{MCM}	$\sqrt{\quad}$	1	$\sqrt{\quad}$	$\sqrt{\quad}$	1

3.3 The Statistical Characteristics of the $GPGW_{MCM}$ Distribution

Under this section, we generate the GPGW mixture cure model distribution’s moments, moment generating function, quantile function, kurtosis, skewness, and random variables generating function, mean deviations, incomplete moments, and mean deviations. (Selim, 2018).

3.3.1 The quantile functions

The quantile function is an option available to the pdf and CDF for describing the distribution of random variables. The quantile function is frequently used to compute statistical measures like the median, skewness, and kurtosis, as well as to generate random variables. The real solution of the given equation is defined as the q^{th} quantile (Kilai, et al., 2022), (Dhungana & Kumar, 2022).

$$F(t_q) = q, 0 \leq q \leq 1 \tag{10}$$

As a consequence, the quantile function $Q(q)$ for GPGW distribution is,

$$Q(q) = \xi^{-\frac{1}{\phi}} \left\{ \left[1 - \frac{\ln\left(\frac{\zeta-q}{1-\zeta}\right)^{1/\omega}}{\beta} \right] - 1 \right\}^{1/\phi} \tag{11}$$

The median $M(t)$ of GPGW – MCM can be obtained by setting $q = 0.5$, to the previous function II,

$$M(t) = \xi^{-\frac{1}{\phi}} \left\{ \left[1 - \frac{\ln\left(\frac{\zeta-0.5}{1-\zeta}\right)^{1/\omega}}{\beta} \right] - 1 \right\}^{1/\phi} \quad (12)$$

3.3.2 Kurtosis and Skewness

The Moors' kurtosis measure based on octiles (Moors, 1988), (Selim, 2018), is provided as;

$$Kurtosis = \frac{Q\left(\frac{7}{8}\right) - Q\left(\frac{5}{8}\right) + Q\left(\frac{3}{8}\right) - Q\left(\frac{1}{8}\right)}{Q\left(\frac{6}{8}\right) - Q\left(\frac{2}{8}\right)} \quad (13)$$

And kurtosis and skewness measurements are used in statistical to characterize a distribution or a data set. Bowley's skewness is a quantile-based measure. (Kenney & Keeping, 1962), (Selim, 2018), (Kilai et al., 2022) is obtained by;

$$Skewness = \frac{Q\left(\frac{3}{4}\right) - 2Q\left(\frac{1}{2}\right) + Q\left(\frac{1}{4}\right)}{Q\left(\frac{3}{4}\right) - Q\left(\frac{1}{4}\right)}$$

The quantile-based skewness and kurtosis measures, such as and Moors' kurtosis, and Bowley's skewness, have several advantages over the classical measures, including being less sensitive to outliers and being available for distributions with no defining moments (Selim, 2018).

3.3.3 Creating random variables

The GPGW distribution's quantile function has a closed form, which makes simulation easier. As a consequence, the following function directly generates the random variables of the GPGW distribution. Where ϕ, β, ξ and ω are recognized parameters, and μ is a Uniform (0, 1) (Selim, 2018).

3.3.4 The moment

If X has the GPGW distribution, then the r^{th} moment for integer value of $\frac{r}{\phi}$ is;

$$\mu'_r = \beta e^\beta \xi^{-\frac{1}{\phi}} \sum_{j=0}^{\frac{r}{\phi}} \frac{(-1)^{j+\frac{r}{\phi}} \left(\frac{r}{\phi}\right)}{\beta^{\frac{1}{2}+1}} \Gamma\left(\frac{j}{\omega}, 1, \beta\right) \quad (13)$$

When $\beta = 1$, the moment of the Nikulin Haghghi distribution is as follow;

$$\mu'_r = \xi^{-\frac{1}{\phi}} \sum_{j=0}^{\frac{r}{\phi}} (-1)^{j+\frac{r}{\phi}} \left(\frac{r}{\phi}\right) \Gamma\left(\frac{j}{\omega}, 1, 1\right) \quad (14)$$

Which is consistent with the results obtained by (Nadarajah & Haghghi, 2011).

The first μ'_1 and second μ'_2 moments, as well as the variance of T, can be calculated As follow;

$$\mu'_1 = E(T) = \beta e^\beta \xi^{-\frac{1}{\phi}} \sum_{j=0}^{\frac{1}{\phi}} \frac{(-1)^{j+\frac{1}{\phi}}}{\beta^{1/\omega+1}} \binom{\frac{r}{\phi}}{j} \Gamma\left(\frac{j}{\omega}, 1, \beta\right) \quad (15)$$

$$\mu'_2 = E(T^2) = \beta e^\beta \xi^{-\frac{2}{\phi}} \sum_{j=0}^{\frac{2}{\phi}} \frac{(-1)^{j+\frac{2}{\phi}}}{\beta^{1/\omega+1}} \binom{\frac{r}{\phi}}{j} \Gamma\left(\frac{j}{\omega}, 1, \beta\right) \text{Var}(T) = \mu'_2 - [\mu'_1]^2 \quad (16)$$

Respectively. As shown below, the non-central in 15 can also be used to calculate the central moment's μ_r and cumulants k_r .

$$\mu_r = \sum_{k=1}^{r-1} (-1)^k \binom{r}{k} \mu_1^{rk} \mu_{r-k} \quad (17)$$

And

$$k_r = \mu'_r = \sum_{k=1}^{r-1} (-1)^k \binom{r-1}{k-1} k_r \mu'_{k-1} \quad (18)$$

Cumulants k_r are quantities that can be used instead of distribution moments. Based on

Cumulants in the forms, the skewness γ_1 and kurtosis γ_2 can be calculated $\gamma_1 = \frac{k_3}{k_2^{3/2}}$

And $\gamma_2 = \frac{k_4}{k_2^2}$ respectively.

3.3.5 The moment generating function

If X GPGW distribution, then the moment generating function is for any integer value $\frac{k}{\phi}$

$$M_z(t) = \beta e^\beta \xi^{-\frac{r}{\phi}} \sum_{r=0}^{\infty} \sum_{j=0}^{\infty} \frac{(-1)^{j+\frac{r}{\phi}} t^r}{\beta^{1/\omega+1} r!} \binom{\frac{r}{\phi}}{j} \Gamma\left(\frac{j}{\omega}, 1, \beta\right) \quad (19)$$

4. ANALYSIS OF RELIABILITY

This section determines the survival function S (t), failure rate function h (t), reversed hazard function R (t), and cumulative failure rate function H (t) for the GPGW distribution.

The Survival Function

The cumulative distribution function in 1 can be used to derive the GPGW distribution's survival function R (t) (Lai, 2014).

$$S(t) = 1 - F(t) = \left[e^{1-(1+\xi z^\phi)^\omega} \right]^\beta, t > 0 \quad (20)$$

4.1 The hazard functions

At any time, the hazard function ($h(t)$) for a continuous distribution with pdf and CDF is de-scribed as follows;

$$h(t) = \frac{P(t < T_1 \leq t + \Delta t | T_1 > t)}{\Delta t} = \frac{f(t)}{S(t)} = \frac{f(t)}{1-F(t)} \quad (21)$$

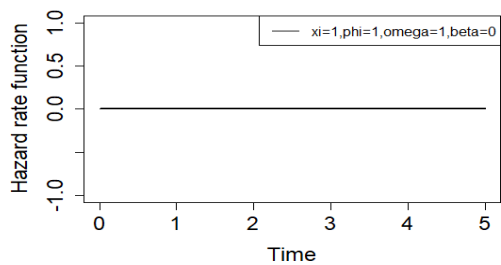
Following that, the $h(t)$ for any time of the GPGW distribution can be determined through the CDF and pdf given in equation 5 and 7 (Selim, 2018) as follows;

$$h(t) = \phi \xi \omega \beta t^{\phi-1} (1 + \xi t^\phi)^{\omega-1}, t > 0 \quad (22)$$

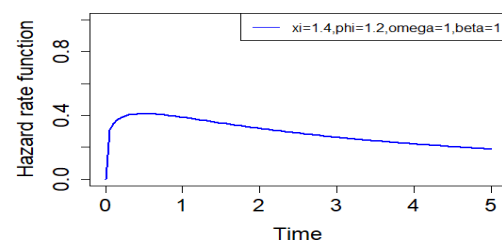
4.2.1 The increasing, decreasing, bathtub, and unimodal failure rate of the GPGW

Monotone increasing when either $\phi > 1$ and $\phi = 1$ or $\omega \phi > \omega > 1$. Monotone decreasing when either $\phi < 1$ and $\omega < 1$ or $\phi \omega = 1$ or $\omega < 1$. Bathtub is when $0 < \phi < 1$ and $\phi \omega > 1$. Unimodal (inverted bathtub shaped) if both $\phi > 1$ and $0 < \phi \omega < 1$. Constant if $h(t) = \beta \xi$ if $\phi = \omega = 1$ (Lai, 2014). Such plots show the $h(t)$'s are flexibility, which makes it valuable and appropriate for non-monotone hazard behaviors that are most probable to be detected in real-world situations (Lai, 2014).

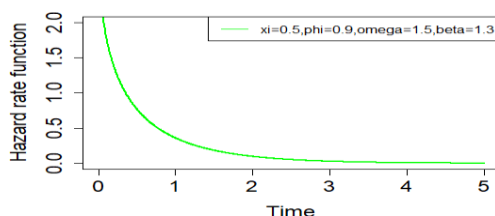
A graphical method based on the TTT, Figure 2, transforms presented by (Barlow & Campo, 1975) (Carrasco et al., 2008) will be used as a tool to demonstrate the variability of the hazard rate shape for a given data set. If the empirical TTT transform is convex, concave, concave then convex, or concave then concave, the shapes of the corresponding hazard rate function for such failure data are decreasing, increasing, bathtub, and unimodal, respectively (Carrasco et al., 2008), (Bidram et al., 2015), (Cooray, 2006)



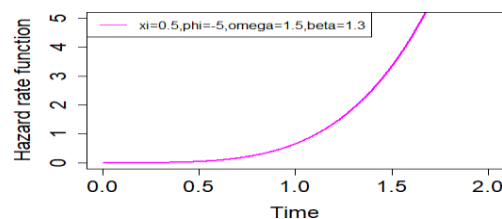
(a) Constant hazard



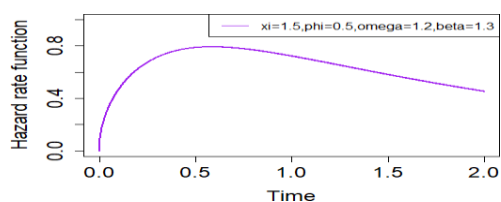
(b) inverse bathtub



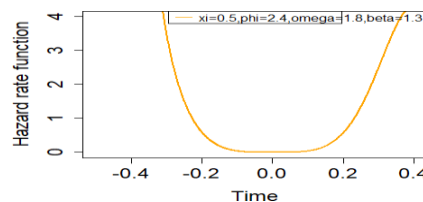
(c) Non monotonic decreasing hazard



(d) Non monotonic increasing hazard

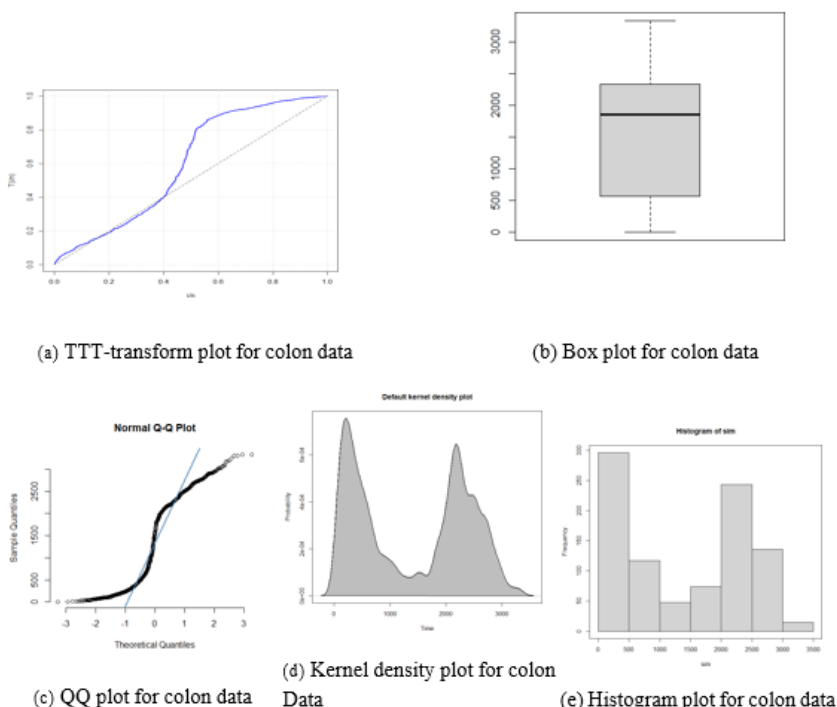


(e) Modified Bathtub inverse



(f) Bathtub

Figure 1: Plots of the hazard function of the GPGW distribution for various parameter values.



(a) TTT-transform plot for colon data

(b) Box plot for colon data

(c) QQ plot for colon data

(d) Kernel density plot for colon Data

(e) Histogram plot for colon data

Figure 2: TTT plot, Boxplot, QQ-plot, and kernel plot and histogram survival time for colon datashown hazard is monotonic.

4.3 Rate functions for the reversed and cumulative hazards

The GPGW distribution’s cumulative hazard rate $H(t)$ and reversed hazard $r(t)$ functions are shown below

$$H(t) = \ln[1 - \exp\{\beta[1 - (1 + \xi t^\phi)^\omega]\}], t > 0 \quad (23)$$

$$r(t) = \frac{\phi \xi \beta \omega t^{\phi-1} (1 + \xi t^\phi)^{\omega-1} [e^{1 - (1 + \xi t^\phi)^\omega}]^\beta}{1 - [e^{1 - (1 + \xi t^\phi)^\omega}]^\beta} \quad (24)$$

4.3.1 Maximum likelihood estimation

Maximum likelihood estimation (MLE) for the GPGW-MCM distribution parameters $\sigma = (\phi, \omega, \beta, \text{ and } \xi)$. is described in this study. Assume that $t_1, t_2, t_3 \dots \dots t_n$ represents a totally random sample of size n drawn from the GPGW-MCM distribution. Following that, the likelihood function is used (Selim, 2018).

$$L(\sigma|t) = ((1 - \zeta)\phi\omega\beta)^n \prod_{i=1}^n t_i^{\phi-1} (\xi t_i^\phi + 1)^{\omega-1} (e^{1-(\xi t_i^\phi + 1)^\omega})^\beta \quad (24)$$

In additional to the log likelihood function (log (L);)

$$\log(L) = n \log((1 - \zeta)\phi\omega\beta) + (\phi - 1) \sum_{i=1}^n \ln t_i + (\omega - 1) \sum_{i=1}^n \ln(\xi t_i^\phi + 1) + \beta - \beta \sum_{i=1}^n (\xi t_i^\phi + 1)^\omega \quad (25)$$

The following are partial derivatives of the preceding equation;

$$\frac{\delta \ln L}{\delta \beta} = \frac{n}{\beta} - \sum_{i=1}^n (\xi t_i^\phi + 1)^\omega + 1 \quad (26)$$

$$\frac{\delta \ln L}{\delta \zeta} = \frac{n}{1+\zeta} \quad (27)$$

$$\frac{\delta \ln L}{\delta \phi} = \frac{n}{\phi} - \sum_{i=1}^n \ln(t_i) + \phi \xi \beta \sum_{i=1}^n \ln(t_i) t_i^\phi (\xi t_i^\phi + 1)^{\omega-1} + (\omega - 1) \xi \sum_{i=1}^n \frac{\ln(t_i t_i^\phi)}{\xi t_i^\phi + 1} \quad (28)$$

$$\frac{\delta \ln L}{\delta \xi} = \frac{n}{\xi} = \omega \beta \sum_{i=1}^n (\xi t_i^\phi + 1)^{\omega-1} + (\omega - 1) \sum_{i=1}^n \frac{t_i^\phi}{\xi t_i^\phi + 1} \quad (29)$$

$$\frac{\delta \ln L}{\delta \omega} = \frac{n}{\omega} - \sum_{i=1}^n (\xi t_i^\phi + 1)^\omega + 1 - \beta \sum_{i=1}^n \ln(\xi t_i^\phi + 1) (\xi t_i^\phi + 1)^\omega \quad (30)$$

The maximum likelihood estimators of $\beta, \omega, \phi, \zeta, \text{ and } \xi$ are the simultaneous solutions of the nonlinear likelihood equation.

The previous equations cannot be solved analytically, but statistical software can solve them numerically using iterative techniques such as the Newton-Raphson algorithm.

5. MONTE CARLO SIMULATION INVESTIGATION (MCMC)

We use an MCMC simulation study in this category to evaluate the performance of parameter estimators for a finite sample of size n. ,(Muhammad et al., 2022),(Alzaghaf et al., 2016) The simulation study was conducted using the generalized power generalized Weibull distribution to determine the biases (BIAS), mean square error (MSE), root mean square error (RMSE),and estimates for the model parameters $\zeta, \phi, \omega, \xi \text{ and } \beta$ The simulation experiment employed a number of simulations with varying sample sizes and parameter values(Muhammad et al., 2022),(Alzaghaf et al., 2016). The quantile function is given in the equation to generate random samples for the GPGW-MCM. The estimations of the GPGW- MCM model are computed using the nlminb, which is an R-function with the method argument set to "BFGS"(generally developed to help improve smoothness) (Muse et al., 2021). The Estimate,

BIAS, RMSE, MSE, Naive SE and CP of the parameters were determined for each piece of simulated data, say $\zeta, \phi, \omega, \xi, \text{ and } \beta$ for $i=1,2,3, n$ (Muse et al., 2021).

$$\text{Bias}(\hat{\psi}) = \frac{1}{N} \sum_{i=1}^N (\hat{\psi} - \psi) \quad (31)$$

$$\text{MSE}(\hat{\psi}) = \frac{1}{N} \sum_{i=1}^N (\hat{\psi} - \psi)^2 \quad (32)$$

$$\text{RMSE}(\hat{\psi}) = \sqrt{\frac{1}{N} \sum_{i=1}^N (\hat{\psi} - \psi)^2} \quad (33)$$

$$\text{NaiveSE} = \frac{\text{Posterior SD}}{\sqrt{n}} \quad (34)$$

$$\text{CP} = \hat{\psi} \mp 1.96 \times \text{SE}(\hat{\psi}) \quad (35)$$

Where $\hat{\psi} = \zeta, \phi, \xi, \omega \text{ and } \beta$ For various sample sizes, Estimations, Bias, and RMSE values of the parameters $\zeta, \phi, \xi, \omega, \text{ and } \beta$ are shown. We indicate, based on these findings, that MCMC- mcm do a good job of estimating model parameters, ensuring that the estimates for these samplesizes are fairly stable and close to the true values (Muse et al., 2021). The posterior mean, Bias, MSE, and RMSE are shown in Table 2. Further to that, the model's parameters' estimations are very close to the true values. As a result, estimates and their asymptotic results can be used to calculate confidence intervals for model parameters even with a small sample size.

6. DATA ANALYSIS

Analytical initiatives are used to examine which distribution fits the information the best. There are four discriminatory practices measures among these analytical initiatives: CAIC (Consistent Akaike Information Criterion), AIC (Akaike Information Criterion), and HQIC (Hannan-Quinn Information Criterion) BIC (Bayesian Information Criterion), (Muse et al., 2021), (Omer et al., 2020)

6.1 Model Choice

The comparisons of mixture cure models based on various distributions The Akaike Information Criteria (AIC) presented by (Suga et al., 2003), The Bayesian Information Criteria (BIC), presented by (Teo et al., 2012), and Hannan Quinn Information Criteria (HQIC) suggested by (Hannan & Quinn, 1979), (Lechman & Popowska, 2020) were used to evaluate data. A lower information criterion value indicates a better model fit (Omer et al., 2020). The AIC, BIC, CAIC, B CAIC and HQIC are defined below.

$$\begin{aligned} \text{AIC} &= 2 \ln[L(\eta)] + 2h, \text{BIC} = -2 \ln[L(\eta)] + h \ln(p) \text{ and } \text{HQIC} = -2 \ln[L(\eta)] + \\ &2h \ln[\ln(p)], \text{BCAIC} = -2 \ln[L(\eta)] + h[\ln(p) + 1], \text{ and } \text{CAIC} = -2 \ln[L(\eta)] + 2h + \\ &[2h \times (h + 1)] / (\eta - \ln[L(\eta)]) \end{aligned} \quad (36)$$

where $L(\eta)$ is the likelihood function h represents the number of free parameters in the model, and p is the number of observations (Beatrice et al., 2022), (Omer et al., 2020). From the table 2, GPGW -MCM has the smallest criterions so is the best fit model for the data.

7. FORMULATION OF A BAYESIAN MODEL

Given a set $t = (t_1 + t_2 + t_3 + \dots + t_n)$ of GPGW data, the model's likelihood function is given by

$$L = \sum_{i=1}^n [v_i \ln \hat{f}(t_i) + (1 - v_i) \ln \hat{S}_i(t_i)] \quad (37)$$

Therefore, the log observed data is where for subject t_i is the observed time (minimum of event and censoring times) and v_i is the indicator that an event has occurred (Li et al., 2010). From equation, 5 and 6, log likelihood is given as;

Table 2: Maximum likelihood results for the GPGW_{MCM} distribution and its sub-models

Models	Parameters	Estimates	AIC	BIC	CAIC	BCAIC	HQIC
	True values						
GPGW _{MCM}	$\beta_0=1$	1.2	6	20.5023	6.0258	20.5023	11.5315
	$\beta=12$	12.14					
	$\zeta=10$	10.26					
	$\omega=1$	1.06					
	$\varphi=3$	3.1					
	$\xi=0.3$	0.3					
PGW _{MCM}	$\beta_0=0.2$	0.2	8	27.3364	8.043	31.3364	15.3754
	$\zeta=10$	10.26					
	$\omega=1$	1.06					
	$\varphi=3$	3.1					
	$\xi=0.3$	0.3					
WMCM	$\beta_0=1$	1.2	10	34.1705	10.0645	39.1705	19.2192
	$\zeta=10.26$	10.26					
	$\varphi=3$	3.1					
	$\xi=0.3$	0.3					
RMCM	$\beta_0=1$	1.2	12	41.0046	12.090	47.0046	23.06
	$\zeta=10.26$	10.26					
	$\xi=0.3$	0.3					
NHMCM	$\beta_0=1$	1.2	7.9	27.3365	8.103	31.34	15.3854
	$\zeta=10$	10.26					
	$\omega=1$	1.06					
	$\xi=0.3$	0.3					

Table 3: Posterior summary of the GPGW mixture cure model distribution, and 1000 samplesize

True Value (θ)	Posterior mean ($\hat{\theta}$)	Posterior properties					\hat{R}	CP
		Bias	Naive SE	MSE	RMSE			
n = 929								
$\beta_0 = 1.2$	1.203	3.95×10^{-3}	2.529×10^{-4}	1.5602×10^{-5}	3.950×10^{-3}	1.02	95.5	
$\beta = -29.14$	-29.1433	3.0426×10^{-3}	1.041×10^{-1}	1.3827×10^{-2}	1.17×10^{-3}	1.00	96	
$\zeta = -0.26$	-0.2555	-4.4158×10^{-3}	5.14×10^{-4}	1.9606×10^{-5}	4.42×10^{-3}	1.05	96.5	
$\omega = -0.06$	-0.069	9.6945×10^{-4}	7.009×10^{-4}	1.3805×10^{-6}	1.17×10^{-3}	1.00	96	
$\phi = -31$	-30.9992	-9.8435×10^{-4}	1.015×10^{-1}	2.30855×10^{-1}	4.80×10^{-1}	1.02	96	
$\xi = 0.0003$	0.00031	-1.0167×10^{-6}	5.098×10^{-7}	2.4417×10^{-12}	1.56×10^{-6}	1.02	95.5	

Table 4: Under non-informative priors, numerical summaries of the posterior properties for the GPGW-MCM model.

Characteristics	Parameters						
	β_0	β	ζ	ω	ϕ	ξ	
Mean	1.203	-29.143	-0.2555	-0.0609	-30.99	0.0003	
Naive SE	0.00025	0.104	0.000051	0.00071	0.1015	5.09×10^7	
Time Series SE	0.0023	0.17	0.0012	0.00149	0.07	5.15×10^6	
Variance	0.0019	325.35	0.0079	0.0147	309.05	0.00001	
Skewness	0.0831	-1.0267	-0.033	-1.0021	-1.049	0.729	
Mode	1.21	-15	-0.275	-0.075	-15	0.0003	
Kurtosis	-0.0483	1.004	-0.03516	-0.5188	1.0009	0.698	
Minimum	1.059	-120.44	-0.634	-0.5188	-127.504	1×10^4	
SD	0.0438	18.04	0.089	0.1214	17.58	8.83×10^5	
Maximum	1.3568	-3.447	0.0791	0.4757	-6.339	0.0008	
Median	1.201	-25.338	-0.2554	-0.0607	-27.181	0.00029	
25 percentile	1.12	-72.3	-0.4317	-0.298	73.9	1.59×10^4	
Q1	1.17	-39.97	-0.315	-0.143	-41.1	2.37×10^4	
Median	1.2	-25	-0.255	-0.0607	-27.07	2.88×10^4	
Q3	1.23	-14.8	-0.19	-0.0212	-17.07	3.55×10^4	
97 percentile	1.29	-6.3416	-0.084	0.1759	-9.1204	5×10^4	

Table 5: chains, each with 9000 iterations (first 1000 discarded)

Parameters	<u>mu.vect</u>	SE	<u>sd.vect</u>	25%	25%	50%	75%	97.5%	\hat{R}	<u>n.eff</u>
$\beta = \zeta$	-0.196	0.002	0.053	-0.294	-0.232	-0.196	-0.161	-0.091	1.01	2000
β_0	0.6825	0.009	0.3038	1.052	4.777	6.736	8.911	12.919	1.01	2000
ω	7.968	0.007	0.202	7.562	7.830	7.968	8.106	8.355	1.02	880
ϕ	-0.001	0.0001	0.002	-0.006	-0.003	-0.001	0.000	0.003	1.02	1100
ξ	-0.042	0.002	0.068	-0.185	-0.085	-0.039	0.003	0.083	1.01	2000
deviance	32225.4	0.1	5.273	32215.7	32221.8	32225.106	32228.8	32236.3	1.01	2000

n. eff is a rough measure of effective sample size for each parameter, and \hat{R} is the potential scale reduction factor (at convergence, $\hat{R} = 1$). DIC information (using the rule, $pD = \text{var}(\text{deviance})/2$) $pD = 13.9$ and $DIC = 32239.3$ (lower deviance is better).

7.1 Visual Convergence Diagnostic of the Real Data

We assessed the convergence of the MCMC algorithm for the proposed models and their special cases (Nakhaei, et al.,2021),(Omer et al., 2020) using both numerical and visual methods. The MCMC algorithm GPGW-MCM has converged to the joint posterior distribution, as shown by the summary results in the above table, because the potential scale reduction factor R is 1, the trace plots mixed well, the correlation between the parameters is minimal, the effective sample size (n.eff) is greater than 400, and the Monte Carlo error (SE) is less than 5% of the posterior standard deviations for all parameters. (Muse et al., 2022), (Omer et al., 2020).

7.2 Trace plot

A trace plot is necessary for evaluating convergence and diagnosing chain problems (Nakhaei et al., 2021). It essentially depicts the sampling process's time series, with the expected result being "white noise"(Nakhaei et al., 2021) Aside from being a useful tool for assessing within chain convergence, the use of different colors for each chain facilitates chain comparison.

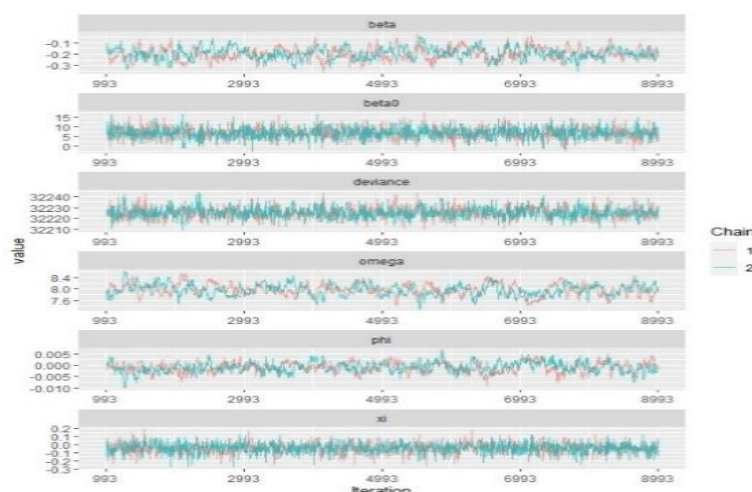
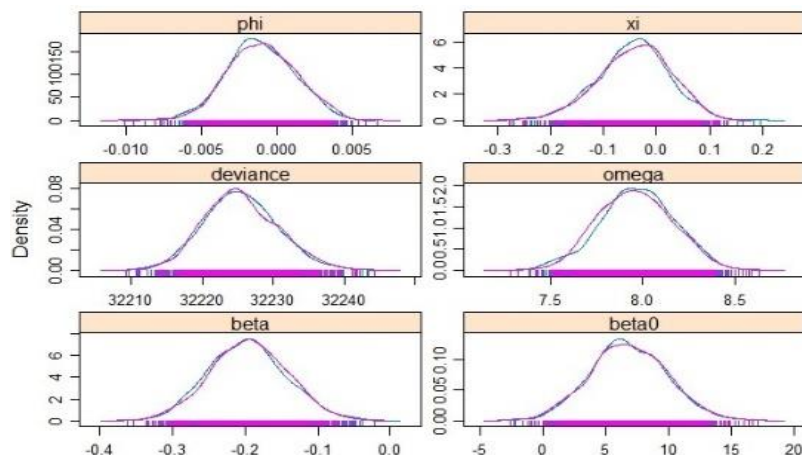


Figure 3: These plots appear to show good "mixing" of the two chains, so we usually say that good mixing should resemble "fuzzy caterpillars."

7.2.1 Density plot

Generates overlapped density plots with various colors for each chain, allowing you to compare the target distribution and whether each chain has converged in a similar space.

Figure 4: Look for sufficient overlap between the two densities



7.2.2 Running means plot

ggs running returns a time series of the chain’s running mean, allowing you to see whether the chain is moving quickly or slowly toward its distribution with specificity (Nakhaei et al., 2021). The comparison is aided by a horizontal line containing the mean of the chain. Using the same scale in the vertical axis allows you to compare chain convergence. In addition to all chains having the same mean, the intended result is a line that is close to the average mean immediately. (Which is easily accessed through the comparison of the horizontal lines)(Nakhaei et al., 2021).

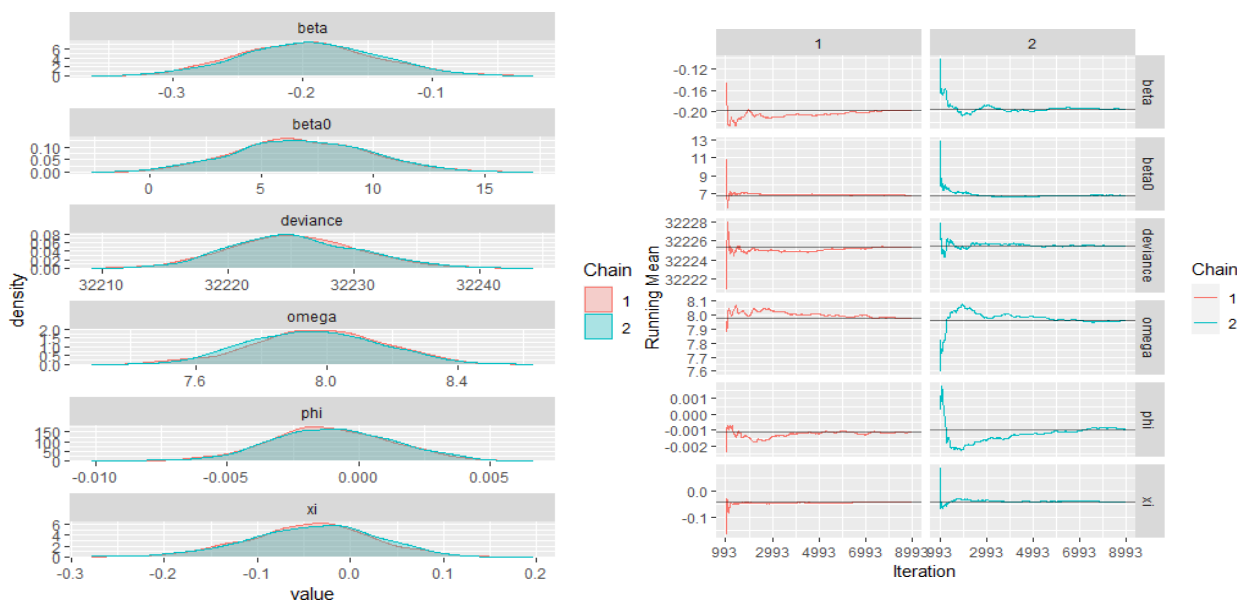


Figure 5: Running Plots, for each chain, display each posterior draw per iteration by variable. The dark line in this plot represents the chain’s posterior mean.

7.2.3 Gelman Diagnostic

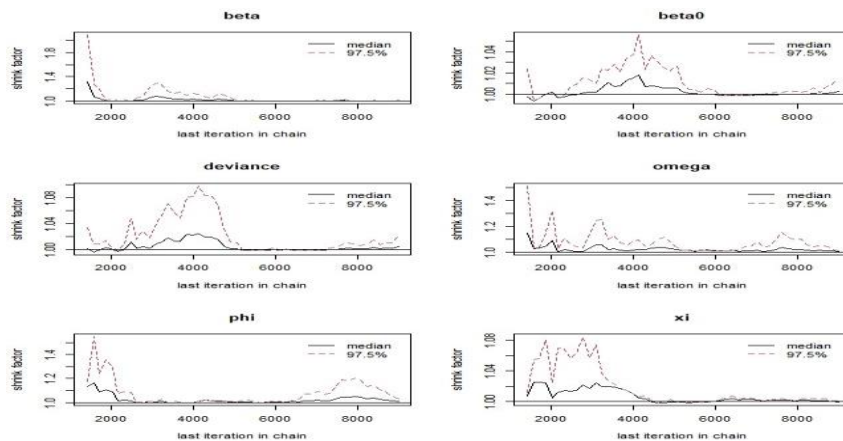
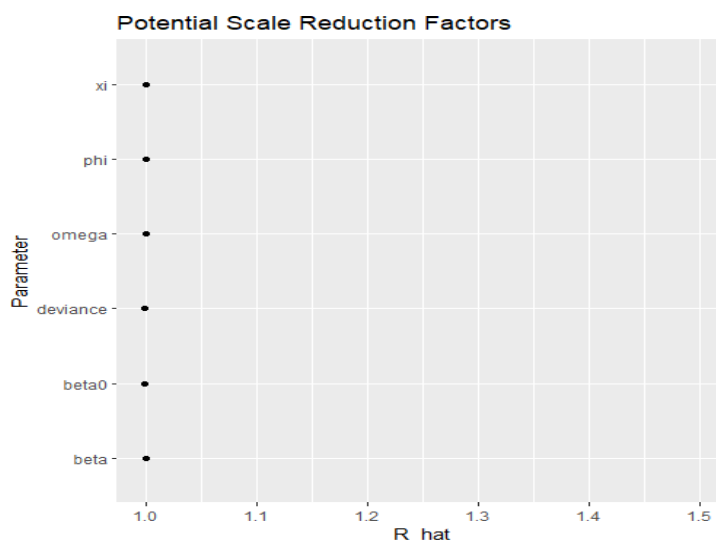


Figure 6: Gelman Diagnostic plots.

Figure 7: The Potential Scale Reduction Factor (R) (Gelman et al. 2003) is based on comparing between-chain variation with within-chain variation for the same parameter. It is expected to be near 1.



7.2.4 Geweke Diagnostic plots

(Geweke, 1992) created a diagnostic that compares the location of the sampled parameter on two different time intervals. For example, if the mean of the first is mean values of the parameter in the two-time intervals is very close to each other, it is assumed that the two unlike parts of the chain are in the same location in the state space.

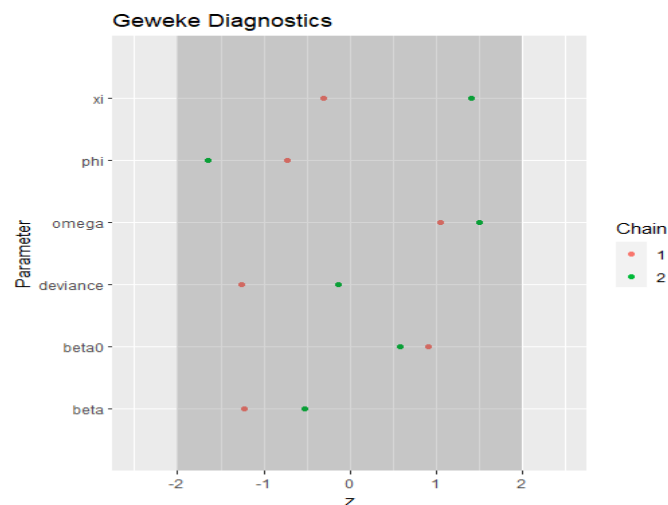


Figure 8: The Geweke z-score diagnostic, on the other hand, compares the first and last parts of the chain. It is also considered a frequentist mean comparable, with 95% of the values falling between -2 and 2. Through default, the area between -2 and 2 is highlighted for faster investigation of difficult chains.

7.2.5 Auto correlation plots

The auto correlation plot predicts a bar at one in the first lag but no auto correlation after that. While auto correlation is not a signal of lack of convergence in and of itself, it may indicate some misbehavior of several chains or parameters, or that a chain requires more time converge. Thinning the chain is the simplest way to solve auto correlation problems (Nakhaei et al., 2021). The auto correlation plot can be used to easily extract the thinning interval. Because the auto correlation axis is bounded by default between -1 and 1, all subplots are comparable. The nLags argument specifies the number of lags to plot, which is set to 50 by default (Nakhaei et al., 2021).

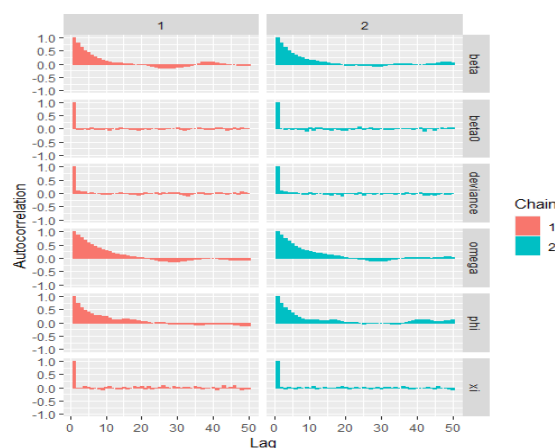


Figure 9: Auto correlational plot diagnostic of the parameter's convergence

7.2.6 Histogram plots

Although it is not a convergence plot, it is useful for providing a quick overview of the value distribution and the shape of the posterior distribution.

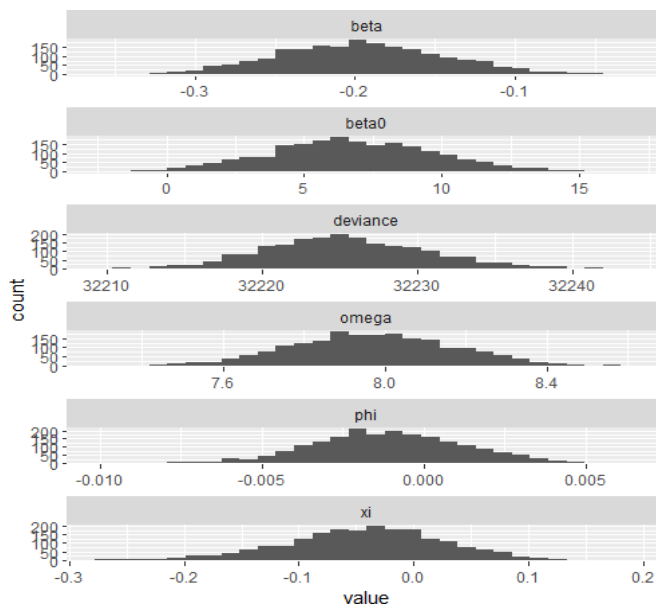
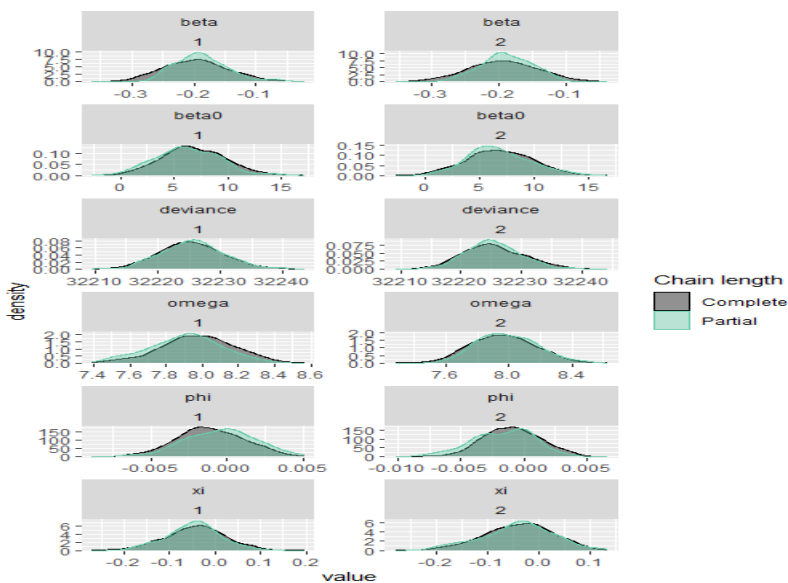


Figure 10: The graph combines the values from all of the chains.

7.2.7 Posterior estimates (Density plots) that contrast the distribution of the entire chain with only the last part of it.

Figure 11: A posterior estimate for comparing the entire chain to the most recent segment.



Posterior estimates, generates overlapped density plots that correlate the last part of the chain (by default, the last ten percent of the values are colored green.) with the entire chain with the entire chain based on the concept of overlapping densities (black). The initial and final parts of the chain should ideally be sampling from the same utilized distribution, so that the overlapped densities are similar. Because the colliding/overlapping densities belong to the same chain, the different columns of the plot correspond to the different chains (Nakhaei et al., 2021).

7.2.8 The correlation between the posterior mean

ggs cross correlation generates a tile plot 13 with the correlations between all parameters to diagnose potential convergence problems caused by highly correlated parameters. The absolute scale argument specifies whether the scale must be between -1 and +1 (Nakhaei et al., 2021). The absolute scale is used by default, which puts the cross correlation issues in context. However, in cases where cross correlation between parameters is not a major issue, using relative scales to identify the most problematic parameters may be useful.

7.2.9 Paired plots

The ggs pairs function in the package ggally makes it simple to extend gg-mcmc by displaying scatter plots 14 of the pairs of parameters in the ggs object, densities, and cross correlations in a single layout. In the plot, the lower argument to ggs pairs is passed as a list to gg pairs, resulting in contours rather than scatter plots in the lower quadrant (Nakhaei et al., 2021).

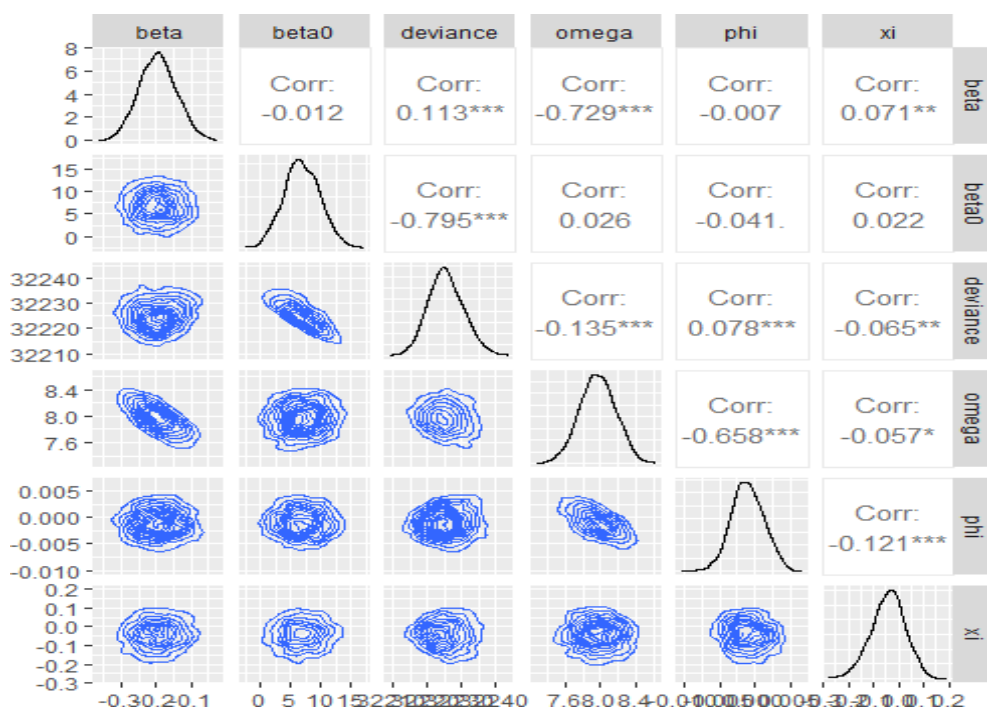


Figure 12: The scatter/contour plots between all pairs of these variables are used to represent the pairs plot.

8. CONCLUSION

The statistical and mathematical properties of the GPGW-MCM were introduced in this paper. The quantile function and its associated results were observed, as well as moments and their associated results and central moments. When the data was uncensored or complete, we just regarded Bayesian and frequentist inference of the suggested distribution's uncertain parameters. The Gibbs sampling procedure and independent gamma priors on the scale and shape parameters are used to generate the Bayesian estimates. Bayesian estimates clearly outperform maximum likelihood estimates only when prior information is accessible. Monte Carlo simulations are used to evaluate estimator attitudes, difference convergence plots, and posterior distributions.

The information criterion of sub-models was examined, as a result, we conclude that among the distributions considered, the GPGW-MCM is the most appropriate model. The GPGW-MCM distribution could also be helpful in research incorporating survival models such as multiple states, accelerated failure time competing risks, and longitudinal data, frailty, and joint survival models.

Availability of data

The data used to support the findings of this study are included within the article.

Conflicts of interest

There are no potential conflicts of interest, according to the author.

Acknowledgements

I would like to thank Prof. Samuel Mwalili and Prof. George Orwa for their thoughtful comments and consultations. Pan African University's Institute for Basic Sciences, Technology, and Innovation for supporting this project.

References

- ❖ Alzaghal, A., Ghosh, I., & Alzaatreh, A. (2016). On shifted Weibull-pareto distribution. *Int. J. Stat. Probab*, 5, 139–149.
- ❖ Bagdonavicius, V., & Nikulin, M. (2001). *Accelerated life models: modeling and statistical analysis*. Chapman and Hall/CRC.
- ❖ Barlow, R. E., & Campo, R. (1975). Total time on test processes and applications to failure data analysis. In *Reliability and fault tree analysis*.
- ❖ Beatrice, N., Amin, Samuel, M., Musili, & George, O., Otieno. (2022). Bayesian estimation of the colon cancer frailty hazards functions for mixture cure model. *Global Scientific Journal*, 10(Issue 6, June 2022), 20.
- ❖ Bidram, H., Alamatsaz, M. H., & Nekoukhou, V. (2015). On an extension of the exponentiated Weibull distribution. *Communications in Statistics-Simulation and Computation*, 44(6), 1389–1404.
- ❖ Carrasco, J. M., Ortega, E. M., & Cordeiro, G. M. (2008). A generalized modified Weibull distribution for lifetime modeling. *Computational Statistics & Data Analysis*, 53(2), 450–462.

- ❖ Cooray, K. (2006). Generalization of the Weibull distribution: the odd Weibull family. *Statistical Modelling*, 6(3), 265–277.
- ❖ De Pascoa, M. A., Ortega, E. M., & Cordeiro, G. M. (2011). The Kumaraswamy generalized gamma distribution with application in survival analysis. *Statistical methodology*, 8(5), 411–433.
- ❖ Dhungana, G. P., & Kumar, V. (2022). Exponentiated odd Lomax exponential distribution with application to covid-19 death cases of Nepal. *PloS one*, 17(6), e0269450.
- ❖ Geweke, J. (1992). Evaluating the accuracy of sampling-based approaches to the calculations of posterior moments. *Bayesian statistics*, 4, 641–649.
- ❖ Gupta, R. C., Gupta, P. L., & Gupta, R. D. (1998). Modeling failure time data by lehman alternatives. *Communications in Statistics-Theory and methods*, 27(4), 887–904.
- ❖ HAGHIGHI, M. N.-F. (2009). On the power generalized Weibull family: model for cancer censored data. *Metron*, 67(1), 75–86.
- ❖ Hannan, E. J., & Quinn, B. G. (1979). The determination of the order of an autoregression. *Journal of the Royal Statistical Society: Series B (Methodological)*, 41(2), 190–195.
- ❖ Kenney, J., & Keeping, E. (1962). Kurtosis. *Mathematics of Statistics*, 3, 102–103.
- ❖ Kilai, M., Waititu, G. A., Kibira, W. A., Abd El-Raouf, M., & Abushal, T. A. (2022). A new versatile modification of the Rayleigh distribution for modeling covid-19 mortality rates. *Results in Physics*, 35, 105260.
- ❖ Lai, C.-D. (2014). Generalized weibull distributions. In *Generalized Weibull distributions* (pp. 23–75). Springer.
- ❖ Lechman, E., & Popowska, M. (2020). Enhancing women’s engagement in economic activities through information and communication technology deployment: Evidence from central–eastern European countries. *Gender, Technology and Development*, 24(3), 314–340.
- ❖ Li, Y., Wileyto, E. P., & Heitjan, D. F. (2010). Modeling smoking cessation data with alternating states and a cure fraction using frailty models. *Statistics in medicine*, 29(6), 627–638.
- ❖ Moors, J. (1988). A quantile alternative for kurtosis. *Journal of the Royal Statistical Society: Series D (The Statistician)*, 37(1), 25–32.
- ❖ Muhammad, M., Liu, L., Abba, B., Muhammad, I., Bouchane, M., Zhang, H., & Musa, S. (2022). A new extension of the top-pleone-family of models with applications to real data. *Annals of Data Science*, 1–26.
- ❖ Muse, A. H., Chesneau, C., Ngesa, O., & Mwalili, S. (2022). Flexible parametric accelerated hazard model: Simulation and application to censored lifetime data with crossing survival curves. *Mathematical and Computational Applications*, 27(6), 104.
- ❖ Muse, A. H., Mwalili, S., Ngesa, O., Almalki, S. J., & Abd-Elmougod, G. A. (2021). Bayesian and classical inference for the generalized log-logistic distribution with applications to survival data. *Computational intelligence and neuroscience*, 2021.
- ❖ Nadarajah, S., & Haghighi, F. (2011). An extension of the exponential distribution. *Statistics*, 45(6), 543–558.
- ❖ Nakhaei, N., Bekker, A., Arashi, M., & Ley, C. (2021). Coming together of bayesian inference and skew spherical data. *Frontiers in big Data*, 129.
- ❖ Nikulin, M., & Haghighi, F. (2006). A chi-squared test for the generalized power Weibull family for the head-and-neck cancer censored data. *Journal of Mathematical sciences*, 133(3).

- ❖ Omer, M. E. A. M. E., Bakar, M. R. A., Adam, M. B., & Mustafa, M. S. (2020). Cure models with exponentiated Weibull exponential distribution for the analysis of melanoma patients. *Mathematics*, 8(11), 1926.
- ❖ Peña-Ramírez, F. A., Guerra, R. R., Cordeiro, G. M., & Marinho, P. R. (2018). The exponentiated power generalized Weibull: Properties and applications. *Anais da Academia Brasileira de Ciências*, 90, 2553–2577.
- ❖ Selim, M. A. (2018). The generalized power generalized Weibull distribution: Properties and applications. arXiv preprint arXiv:1807.10763.
- ❖ Suga, R., Yonekawa, K., & Kawahara, M. (2003). Estimation of tidal current using kalman filter finite element method with aic. In *Computational fluid and solid mechanics 2003* (pp. 1821–1825). Elsevier.
- ❖ Teo, B. W., Xu, H., Koh, Y. Y., Li, J., Sinha, A. K., Shuter, B., ... Lee, E. J. (2012). Estimating kidney function in a multiethnic Asian population with multiple filtration markers. *American Journal of Kidney Diseases*, 60(3), 500–502.
- ❖ Xi, Y., & Xu, P. (2021). Global colorectal cancer burden in 2020 and projections to 2040. *Translational Oncology*, 14(10), 101174.
- ❖ Zhang, T., & Xie, M. (2007). Failure data analysis with extended Weibull distribution. *Communications in Statistics—Simulation and Computation*.